

## Effect of projectile ground state spin on fission fragment anisotropies in $^{10}\text{B}$ , $^{11}\text{B}+^{232}\text{Th}$ reactions

B. K. Nayak,<sup>1</sup> R. G. Thomas,<sup>1</sup> R. K. Choudhury,<sup>1</sup> A. Saxena,<sup>1</sup> P. K. Sahu,<sup>1</sup> S. S. Kapoor,<sup>1</sup> Raghav Varma,<sup>1,2</sup> and D. Umakanth<sup>1,3</sup>

<sup>1</sup>Nuclear Physics Division, B.A.R.C., Bombay 400 085, India

<sup>2</sup>Indian Institute of Technology, Powai, Mumbai 400 076, India

<sup>3</sup>Microtron Center, Mangalore University, Mangalore 574 199, India

(Received 11 April 2000; published 15 August 2000)

Fission fragment angular distributions have been measured for  $^{10}\text{B}(\text{spin}=3^+)$ ,  $^{11}\text{B}(\text{spin}=3/2^-)+^{232}\text{Th}$  reactions at projectile energies below and above the Coulomb barrier. The fragment anisotropies for the  $^{11}\text{B}+^{232}\text{Th}$  system are found to be significantly larger than the statistical saddle point model (SSPM) predictions at sub-barrier energies, while for the  $^{10}\text{B}+^{232}\text{Th}$  system the deviations from SSPM predictions are found to be much less. The present results indicate that the ground state spin of the projectile influences the fragment anisotropies at sub-barrier energies in a larger way than predicted by the statistical model with the inclusion of the  $M$ -state distributions. Calculations were carried out based on the entrance channel dependent  $K$ -states distribution and preequilibrium fission models, with inclusion of ground state spin of the projectiles, which are found to explain the variation of fission fragment anisotropies as a function of bombarding energy for both the systems.

PACS number(s): 25.70.Jj, 24.75.+i, 25.85.Ge

Recently, there has been a lot of interest in the study of fission fragment angular distributions in heavy ion induced fission reactions using actinide targets because of the observation of anomalously large fission fragment anisotropies at near- and sub-barrier energies in these systems, as compared to the calculations based on the statistical saddle point model (SSPM) [1,2]. The general conclusion from these studies is that the large ground state deformation of the actinide target nuclei influences the fission process at the sub-barrier energies leading to fission events before full equilibration of the  $K$  degree of freedom (preequilibrium fission), which accounts for the large anomalous fragment angular anisotropies observed in these systems. The projectile deformation, however, does not seem to affect the fission fragment anisotropies, as was evident from the  $^{28}\text{Si}+^{208}\text{Pb}$  reaction, where the fission fragment anisotropies were found to be normal at near- and sub-barrier energies [3]. In a recent study [4], it was shown that for actinide nuclei, the presence of large target ground state spin had an influence on the deviation of the fission fragment anisotropies from SSPM predictions at sub-barrier energies. It was seen that for the  $^{12}\text{C}+^{236}\text{U}$  and  $^{12}\text{C}+^{238}\text{U}$  systems having zero ground state spin, the fragment anisotropies exhibit a large anomaly around Coulomb barrier energies, whereas for the  $^{12}\text{C}+^{235}\text{U}$  system having large ground state target spin, the deviations of the observed fragment anisotropies from SSPM predictions were found to be much less. These results were interpreted in the framework of the entrance channel dependent (ECD)  $K$ -state distribution based on the preequilibrium fission model [5,6] by incorporating the ground state spin of the target in the calculation of the fragment angular distributions. In the case of nonzero ground state target spin ( $I_O$ ) the entrance channel  $K$ -state distribution is not peaked at  $K=0$  but at  $K=\pm I_O$ , which is responsible for lowering the angular anisotropies at sub-barrier energies. If, however, the target nucleus, has zero spin, but the projectile has a spin  $I_O$  and it gets transformed to  $K$  of the dinuclear complex (the spin along the symmetry

axis), then the entrance channel  $K$ -state distribution will also peak at  $K=\pm I_O$ . It is, therefore, of interest to investigate if the ground state spin of the projectile has any influence on the deviations of the fission fragment angular distributions from the SSPM predictions at the sub-barrier energies. It is in this context that in the present Rapid Communication, we have carried out measurements of the fission fragment angular distributions in the  $^{10}\text{B}(I_O=3^+)$  and  $^{11}\text{B}(I_O=3/2^-)+^{232}\text{Th}$  systems over a broad energy range both at above and below barrier energies, to investigate the effect of the projectile ground state spin on the fragment anisotropies. The  $^{10}\text{B}$ ,  $^{11}\text{B}$  induced fission reactions on the  $^{232}\text{Th}$  target have been studied earlier by many authors [7,2,8] and there have been some contradictory results reported in certain cases on the fission fragment anisotropies at the sub-barrier energies. Majumdar *et al.* [2] have reported a large peaklike structure in the anisotropies in  $^{11}\text{B}+^{232}\text{Th}$  reaction, which was not reproduced in the measurements reported by Lestone *et al.* [8]. In order to examine the behavior of the fission fragment anisotropies in the  $^{10}\text{B}$ ,  $^{11}\text{B}$  induced fission reactions on the  $^{232}\text{Th}$  target, we have carried out a consistent set of measurements around Coulomb barrier energies. The results are analyzed to infer the effect of ground state spin of the projectile on the fragment anisotropies in these systems.

The measurements were carried out using the  $^{10}\text{B}$  and  $^{11}\text{B}$  beams obtained from the 14 MV BARC-TIFR pelletron accelerator at Mumbai. A self supporting  $1.8\text{ mg/cm}^2$   $^{232}\text{Th}$  target was used and the fission fragments were detected using two silicon surface barrier detectors of thickness  $17\text{ }\mu\text{m}$  and  $12\text{ }\mu\text{m}$ . The elastic and inelastic-scattering events of the projectile ions were eliminated by taking anticoincidence with a veto detector mounted behind the  $17\text{ }\mu\text{m}$  detector. For the  $12\text{ }\mu\text{m}$  detector, the veto detector was not required, since the fission events were very much separated from the elastically scattered events. The angular distribution measurements were carried out over the laboratory angular range of  $80^\circ-170^\circ$ . The relative solid angles of the two detectors

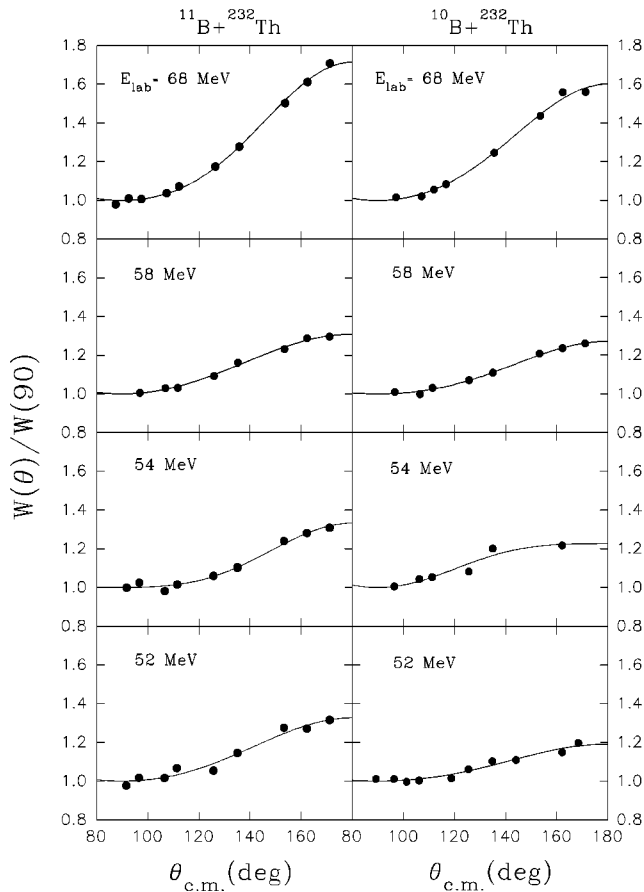


FIG. 1. Measured fragment angular distributions for  $^{10}\text{B}, ^{11}\text{B} + ^{232}\text{Th}$  systems at a few typical bombarding energies. The continuous lines are fits to the data points.

were determined by taking data in both detectors at overlapping angles. The absolute fission cross sections were obtained by normalization to Rutherford scattering with a monitor detector mounted at a forward angle ( $\theta_{lab} = 25^\circ$ ). The measured fragment angular distributions were transformed to the center-of-mass system by assuming symmetric mass division and using the Viola systematics [9] for fragment kinetic energies. For the lighter projectiles of  $^{10}\text{B}$  and  $^{11}\text{B}$ , the contribution from transfer induced fission is expected to be quite insignificant compared to fusion-fission and hence the fission events are assumed to correspond to the fission of compound nucleus formed by the complete fusion of the target and the projectile. Figure 1 shows the fragment angular distributions for the  $^{10}\text{B}, ^{11}\text{B} + ^{232}\text{Th}$  systems at a few typical bombarding energies. The angular distributions were fitted by Legendre polynomials (shown by continuous lines) to derive the angular anisotropy [ $W(180^\circ)/W(90^\circ)$ ] values at various bombarding energies. Figure 2 shows the fragment angular anisotropies for both the reactions as a function of the bombarding energy. It is seen that at a given bombarding energy, the fragment anisotropy is lower for the  $^{10}\text{B} + ^{232}\text{Th}$  system as compared to that of the  $^{11}\text{B} + ^{232}\text{Th}$  system, which is ascribable to the difference in the average angular momenta in the two systems. The results of the SSPM calculations are also shown as dashed lines in Fig. 2. The fission

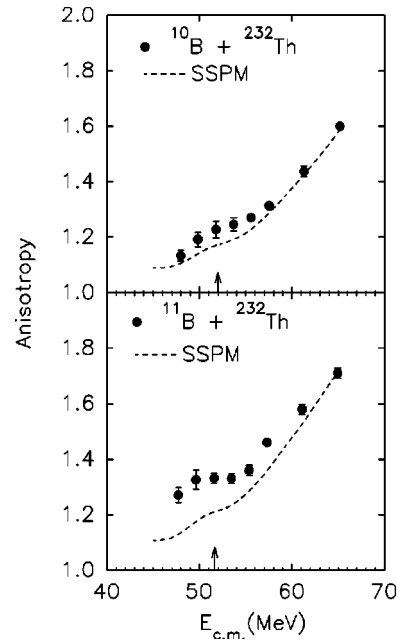


FIG. 2. Experimental and calculated fission fragment anisotropies in SSPM as a function of bombarding energy for  $^{10}\text{B}, ^{11}\text{B} + ^{232}\text{Th}$  systems.

barrier parameters such as the barrier height  $B_f$  and effective moment of inertia  $I_{eff}$  required for the SSPM calculations were taken from the finite range rotating model calculations of Sierk [10]. The compound nucleus  $l$  distributions were calculated using the CCDEF [11] code, which reproduced the measured fission cross sections for both the systems as shown in Fig. 3. The CCDEF calculations were done by taking into account the static deformation of the  $^{232}\text{Th}$  target nucleus ( $\beta_2 = 0.22, \beta_4 = 0.09$ ). The effective temperature at the saddle point was determined after correcting the excitation energy for the energy removed by the pre-scission neutron ( $\nu_{pre}$ ) emissions and using the level density parameter  $a = A/10 \text{ MeV}^{-1}$ . The experimental results on the pre-scission neutron multiplicity as a function of fissility and excitation energy were taken from Ref. [12] for estimating this correction [13]. As the experimental ( $\nu_{pre}$ ) number is only available for the  $^{11}\text{B} + ^{232}\text{Th}$  system, we have assumed a similar excitation energy dependence of  $\nu_{pre}$  for the  $^{10}\text{B} + ^{232}\text{Th}$  system. The  $\nu_{pre}$  numbers are in the range of  $\sim 0.6$  to  $\sim 1.6$  and compound nuclear excitation energies are in the range of  $\sim 31.0 \text{ MeV}$  to  $\sim 50.0 \text{ MeV}$  for the  $^{11}\text{B} + ^{232}\text{Th}$  system. Similarly for the  $^{10}\text{B} + ^{232}\text{Th}$  system,  $\nu_{pre}$  numbers are in the range of  $\sim 0.9$  to  $\sim 2.0$  and compound nuclear excitation energies are in the range of  $\sim 37.0 \text{ MeV}$  to  $\sim 55.0 \text{ MeV}$ . The SSPM calculations were carried out by using the exact expressions [14] for fission fragment angular distributions with proper weighting of  $J$ ,  $M$ , and  $K$  states to take into account the projectile spin. It is seen from Fig. 2 that at energies far above the barrier, the SSPM calculations are able to explain the experimental results, but fail to reproduce the fragment anisotropies at near and below barrier energies. The discrepancy between the calculations and the experiment is found to be more pronounced for the  $^{11}\text{B} + ^{232}\text{Th}$  system at below barrier energies. The present experimental results

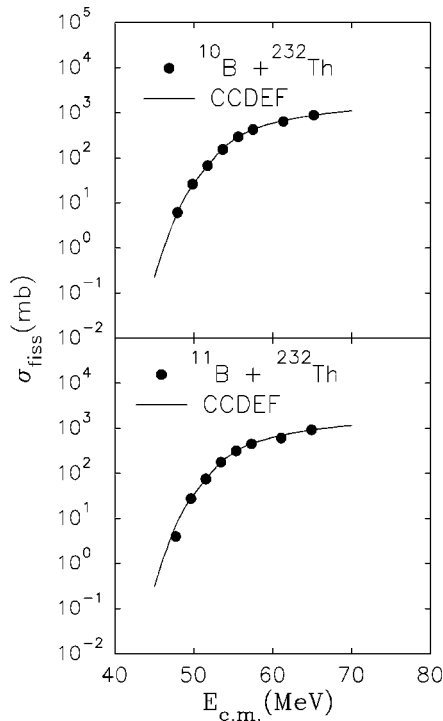


FIG. 3. Comparison between the measured and CCDEF predictions of fission excitation functions for  $^{10}\text{B}$ ,  $^{11}\text{B} + ^{232}\text{Th}$  systems.

on the fission fragment anisotropies in the  $^{11}\text{B} + ^{232}\text{Th}$  reaction, as a function of bombarding energy, do not show the pronounced bump reported by Majumdar *et al.* [2], who have employed fission fragment folding angle distribution measurements for determination of fragment anisotropies. The present results are, however, in agreement with the results reported by Lestone *et al.* [4], who have also carried out singles measurements for fragment anisotropy determination as in the present Rapid Communication. As pointed out above, the target spin effects on the fission fragment anisotropies at sub-barrier energies have been explained earlier in the framework of ECD  $K$ -state distribution based on the preequilibrium fission hypothesis by considering the ground state spin of the targets [4]. In the present Rapid Communication, the target has zero spin but the projectiles  $^{10}\text{B}$  and  $^{11}\text{B}$  have different ground state spins. In order to compare with the experimental results of fragment anisotropy as a function of bombarding energy for the above systems, we have carried out theoretical calculations similar to the ECD model calculations, with the additional assumption that the spin of the projectile gets converted to  $K$  (the spin along the symmetry axis) of the fissioning nucleus. The main ingredient of the ECD model as applied to a deformed target nucleus with spin  $I_0$  is that immediately following fusion the system has the  $K$ -state distribution of the entrance channel and that this initial distribution gets broadened with time due to coupling between intrinsic and collective rotational degrees of freedom. Secondly, the entrance channel  $K$ -state distribution has a strong dependence on the beam energy due to varying transmission coefficients at different contact points in sub-barrier fusion. At above-barrier energies where the contact points are equally probable the entrance channel  $K$

distribution is fairly uniform and broad and thus the  $K$ -state equilibration has little influence on the  $K$ -state distribution of the fissioning system. However, at sub-barrier energies the entrance channel  $K$ -state distribution is peaked at  $K=0$ , and strongly influences the  $K$ -state distribution of the fissioning system. If the target or projectile has a ground state spin  $I_0$ , the entrance channel  $K$ -state distribution is taken to peak at  $K = \pm I_0$  instead of  $K=0$  at near- and sub-barrier energies [4]. As a consequence, if the ground state spin of the target or projectile is large as in the case of  $^{10}\text{B}(3^+)$ , the anisotropy at sub-barrier energies gets reduced and becomes closer to SSPM predictions, whereas for zero or low ground state spins in the entrance channel as in the case of  $^{11}\text{B}(3/2^-)$ , the anisotropy is expected to show deviations from the SSPM predictions.

According to the preequilibrium fission model, the fission  $K$  distribution is given by  $P_f(K) = P_{\text{initial}}(K)P_{\text{saddle}}(K)$ , where  $P_{\text{initial}}(K)$  is the  $K$ -state distribution of the initial dinuclear complex and  $P_{\text{saddle}}(K)$  is the equilibrated Gaussian  $K$  distribution at the saddle point. In the original paper, Ramamurthy and Kapoor [5] had applied their preequilibrium fission model to the case of a spherical target and projectile, where the entrance channel  $K$ -state distribution was assumed to peak at  $K=0$ , since in this case the fission symmetry axis developing along the line joining the centers of the two nuclei, is always perpendicular to  $J$ . This formalism was extended by Vorkapic *et al.* [6], to include the target deformation in the calculation of the entrance channel  $K$ -state distribution. Following the work of [4,6],  $F(J, K, K')$  can be defined as the probability of a fissioning system having the quantum numbers  $J$  and  $K$ , when populated from an entrance channel  $K$ -state distribution which peaks at  $K'$ , and is given by

$$F(J, K, K') = \exp\left[-\frac{(K-K')^2}{2\sigma_K^2}\right] \times \exp\left[-\frac{(K\hbar)^2}{2I_{\text{eff}}T}\right]. \quad (1)$$

$F(J, K, K')$  is obtained by taking the initial  $K$ -state distribution for each  $J$  value convoluted by a Gaussian with standard deviation  $\sigma_K$  and multiplied by the SSPM  $K$ -state distribution at fission saddle. If the target nucleus is oriented by an angle  $\omega$  with respect to the beam direction, the entrance channel  $K$ -state distribution peaks at the most probable value,  $K' = J \sin \omega$ . The entrance channel  $K$ -states population for particular angular momentum value  $J$  is determined from fusion cross section  $\sigma_{\text{fus}}(J, \omega)$  at various target-projectile orientations. If the target or projectile has ground state spin,  $I_0$ , the entrance channel  $K$ -state distribution peaks at  $K' = J \sin \omega \pm I_0$ . Figure 4 shows entrance  $K$ -state distributions calculated for a typical case of  $J = 10\hbar$  for various arbitrary ground state spin values in the  $^{10}\text{B} + ^{232}\text{Th}$  reaction at  $E_{\text{c.m.}} = 47$  MeV (below Coulomb barrier) and  $E_{\text{c.m.}} = 65$  MeV (above Coulomb barrier). As discussed earlier and in Ref. [4], the entrance channel  $K$ -state distribution is nearly uniform for above barrier case of  $E_{\text{c.m.}} = 65$  MeV, while at  $E_{\text{c.m.}} = 47$  MeV the  $K$ -state distributions strongly depend on the ground state spin of the projectile and peak around the value of the ground state spin of the projectile. The equi-

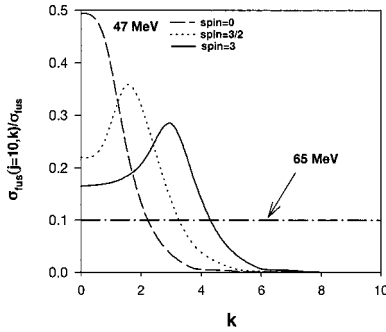


FIG. 4. The entrance channel  $K$ -state distributions calculated for  $J=10\hbar$  at  $E_{c.m.}=65$  MeV and  $E_{c.m.}=47$  MeV for various projectile ground state spin values in the  $^{10}\text{B}+^{232}\text{Th}$  reaction.

bration broadening of the entrance channel  $K$ -state distribution is modeled by defining a width,  $\sigma_K$ , as given by [5]

$$\sigma_K = J\sigma_\theta, \quad (2)$$

where  $\sigma_\theta = q\sqrt{Tt}$ ,  $T$  is the temperature at the saddle point,  $t$  is the time, and  $q$  is a constant [4]. We have taken  $t$  as the Bohr-Wheeler fission time for the determination of  $\sigma_\theta$ . Using Eqs. (1) and (2), and considering all the  $M$  states produced by projectile ground state spin, we obtain the following expression for the fission fragment angular distribution:

$$W(\theta) \propto \sum_J \sum_{M=-I_0}^{I_0} P(M) \sum_\omega \sigma_{fus}(J, \omega) \times \sum_{K=-J}^J \frac{(2J+1)}{4\pi} \frac{|d_{M,K}^J(\theta)|^2 F(J, K, K')}{\sum_{K=-J}^J F(J, K, K')}. \quad (3)$$

$P(M)$  in Eq. (3) is the  $M$ -state probability distribution. Following the prescription given in Ref. [4], we have made a semiclassical estimation of the  $M$ -state distributions using the projection of the ground state spin on the beam axis at the time of fusion ( $M=I_0 \cos \omega$ ) as follows:

$$P(M) = \sum_{J,K} \int \frac{d\sigma_{fus}(J, \omega, K, M)}{d\omega} d\omega. \quad (4)$$

The fission fragment angular distributions were calculated using Eq. (3). Figure 5 shows the results of these calculations (solid lines) for the fission fragment anisotropies for the  $^{10}\text{B}(I_0=3)+^{232}\text{Th}$  and  $^{11}\text{B}(I_0=3/2)+^{232}\text{Th}$  reactions along with the experimental data. The dashed lines are the predictions of SSPM as discussed earlier. The ECD based on preequilibrium model gives a good description of the fission fragment anisotropies observed experimentally for both the systems with the value of  $q$  taken as  $\sim 0.17(\text{MeV}$

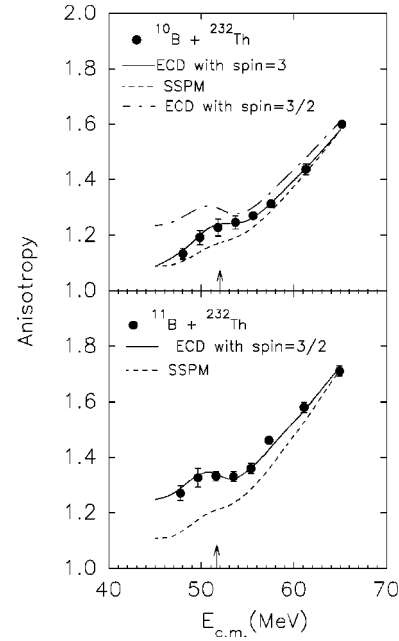


FIG. 5. Experimental and calculated fission fragment anisotropies in SSPM and ECD models as a function of bombarding energy for  $^{10}\text{B}+^{232}\text{Th}$  and  $^{11}\text{B}+^{232}\text{Th}$  systems, respectively.

$\times 10^{-21}\text{s})^{-1/2}$ . In order to examine the sensitivity of the calculations to the value of the ground state spin, we have carried out calculations for the  $^{10}\text{B}$  system using a fictitious spin value of 3/2, and the results are shown in Fig. 5 by the dot-dashed line. The calculations are found to be quite sensitive to the value of spin at the sub-barrier energies. It may be concluded that at the sub-barrier energies, the projectile spin has a large effect on the fragment anisotropy values. The enhancements in the fragment anisotropies over the SSPM predictions in the present systems can be accounted by incorporating the nonequilibrium  $K$ -state distributions suggested by the preequilibrium hypothesis.

In summary, we have measured the fission fragment anisotropies for the  $^{10}\text{B}+^{232}\text{Th}$  ( $I_0=3$ ) and  $^{11}\text{B}+^{232}\text{Th}$  ( $I_0=3/2$ ) systems at near- and sub-barrier energies. The experimental results show that the presence of projectile ground state spin significantly affects the fission fragment anisotropies at sub-barrier energies. The ECD  $K$ -states model based on the preequilibrium fission hypothesis, incorporating the projectile ground state spin, provides a consistent description of the measured fragment anisotropies around Coulomb barrier energies for both the systems.

The authors are thankful to Dr. D. C. Biswas, L. M. Pant, and D. V. Shetty for their helpful contributions to this work. Thanks are also due to the Pelletron staff for their help in providing the required beams from the accelerator.

[1] S. Kailas, Phys. Rep. **284**, 381 (1997).

[2] N. Majumdar *et al.*, Phys. Rev. Lett. **77**, 5027 (1996).

[3] D. J. Hinde, C. R. Morton, M. Dasgupta, J. R. Leigh, J. C. Mein, and H. Timmers, Nucl. Phys. **A592**, 271 (1995).

[4] J. P. Lestone *et al.*, Phys. Rev. C **56**, R2907 (1997).

[5] V. S. Ramamurthy and S. S. Kapoor, Phys. Rev. Lett. **54**, 178 (1985).

[6] D. Vorkapic and B. Ivanisevic, Phys. Rev. C **52**, 1980 (1995).

- [7] V. S. Ramamurthy *et al.*, Phys. Rev. Lett. **65**, 25 (1990).
- [8] J. P. Lestone, A. A. Sonzogni, M. P. Kelly, and R. Vandenbosch, Phys. Rev. Lett. **81**, 4776 (1998).
- [9] V. E. Viola *et al.*, Phys. Rev. C **31**, 1550 (1985).
- [10] A. J. Sierk, Phys. Rev. C **33**, 2039 (1986).
- [11] J. Fernandez-Niello, C. H. Dasso, and S. Landowne, Comput. Phys. Commun. **54**, 409 (1989).
- [12] A. Saxena, A. Chatterjee, R. K. Choudhury, D. M. Nadkarni, and S. S. Kapoor, Phys. Rev. C **49**, 932 (1994).
- [13] A. Saxena, S. Kailas, A. Karnik, and S. S. Kapoor, Phys. Rev. C **47**, 403 (1993).
- [14] R. Vandenbosch and J. R. Huizenga, *Nuclear Fission* (Academic, New York, 1973).